analytical chemistry

pubs.acs.org/ac Article

Functionalized Persistent Luminescence Nanoparticle-Based Aptasensor for Autofluorescence-free Determination of Kanamycin in Food Samples

Bei-Bei Wang, Xu Zhao, Li-Jian Chen, Cheng Yang, and Xiu-Ping Yan*

Cite This: *Anal. Chem.* 2021, 93, 2589−2595 Read Online

ACCESS | Metrics & More | Article Recommendations | Supporting Information

ABSTRACT: Selective and sensitive determination of trace kanamycin in complex food samples is of great importance for food safety because of its high toxicity. Here, we report a sensitive and autofluorescence-free persistent luminescence (PL) aptasensor for selective, sensitive, and autofluorescence-free determination of kanamycin in food samples. The aptamer for kanamycin was first conjugated onto the surface of magnetic nanoparticles Fe_3O_4 to serve as the recognition unit as well as the separation element, while the PL nanoparticles $ZnGa_2O_4$:Cr (PLNPs) were functionalized with the aptamer complementary DNA (cDNA) as the PL signal. The PL aptasensor consisted of the aptamer-conjugated MNPs (MNPs-apt) and cDNA-functionalized PLNPs (PLNPs-cDNA) and combined the merits of the long-lasting luminescence of PLNPs, the magnetic separation ability of MNPs as well as the selectivity of the aptamer, offering a promising approach for autofluorescence-free determination of kanamycin in food samples. The proposed aptasensor showed excellent linearity in the range from 1 pg mL^{-1} to 5 ng mL^{-1} with a limit of detection of 0.32 pg mL^{-1}. The precision for 11 replicate determinations of 100 pg mL^{-1} kanamycin was 3.1% (relative standard deviation). The developed aptasensor was applied for the determination of kanamycin in milk and honey samples with the recoveries of 95.4−106.3%. The proposed aptasensor is easily extendable to other analytes by simply replacing the aptamer, showing great potential as a universal aptasensor platform for selective, sensitive, and autofluorescence-free detection of hazardous analytes in food samples.

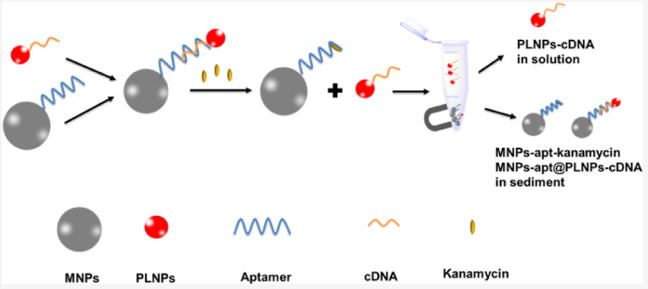

INTRODUCTION

Kanamycin, an important aminoglycoside antibiotic, has been widely used in veterinary medicine for the prevention and treatment of human and food-producing animal microbial infections or as dietary supplements in livestock husbandry.[1−4] The irrational use of kanamycin easily leads to residue in food products. Most of kanamycin can be metabolized, but not completely; thus, trace amounts of kanamycin accumulate in human body by food chain threatening human health.[5−7] It is necessary to maintain the content of kanamycin below the maximum residue limit. The European Union has established a maximum allowable kanamycin level of 150 $\mu g\ kg^{-1}$ in milk and 100 $\mu g\ kg^{-1}$ in pork.[8,9] Till now, quite a few methods have been developed for the determination of kanamycin based on high-performance liquid chromatography,[10] surface-enhanced Raman scattering,[11] fluorescence,[12] enzyme-linked immunosorbent assay,[13,14] and electrochemical immunosensor.[15−17] The fluorescence method is favored by researchers because of its high sensitivity, simplicity, and flexible design. However, most of the fluorescent methods need constant light excitation to generate fluorescent signals and thus suffer autofluorescence interference from the sample matrix. Therefore, it is imperative to develop a sensitive and selective method for autofluorescence-free determination of kanamycin in complicated samples.

Various methods based on X-ray scintillating nanotags and persistent luminescent nanoprobes have been developed to eliminate autofluorescence interference.[18−26] Persistent luminescence (PL) refers to the phenomenon, whereby luminescence lasts for minutes, hours, or days after stopping excitation.[20,21] Therefore, PL nanoparticles (PLNPs) enable PL detection without the need for in situ excitation, thus permitting autofluorescence-free detection. Functionalized PLNP-based probes with no requirement for in situ excitation during detection provides many advantages in autofluorescence-free detection, making PLNPs attractive for biosensing and bioimaging.[22−26] However, the application of PLNPs in the analysis of food samples for hazardous analytes is still rare.

Received: November 3, 2020
Accepted: December 23, 2020
Published: January 7, 2021

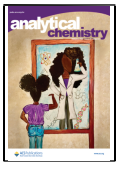

https://dx.doi.org/10.1021/acs.analchem.0c04648
Anal. Chem. 2021, 93, 2589−2595

Considering the complex food matrix (high amounts of fat, oil, starch, protein, or sugar), the matrix components such as sugar and protein may interfere with the detection of the fluorescence signal under ultraviolet excitation.[27] Besides, the concentration of target compounds such as the antibiotic residue is usually lower than nanograms per gram.[28,29] Therefore, sensitive analytical methods are particularly important. PLNPs can efficiently eliminate the interferences from the autofluorescence of the food complex matrix and light scattering as there is no need for in situ excitation, which leads to significant improvement of the signal-to-noise ratio.

In this work, we show a PL-based aptasensor for sensitive and autofluorescence-free determination of kanamycin in food samples. To fabricate the aptasensor, magnetic nanoparticles Fe_3O_4 (MNPs) are functionalized with the aptamer for kanamycin as the recognition unit as well as the separation element. Meanwhile, $ZnGa_2O_4$:Cr PLNPs is explored as the luminescence source because of the long NIR-persistent emitting. The aptamer complementary DNA (cDNA) is then grafted onto the surface of the PLNPs to give cDNA-functionalized PLNPs (PLNPs-cDNA). The aptamer-modified MNPs (MNPs-apt) then hybrids with PLNPs-cDNA to give a PL turn-on aptasensor MNPs-apt@PLNPs-cDNA for kanamycin. MNPs-apt enable selective capture of kanamycin and rapid separation from sample solution. The developed aptasensor offers the combined merits of no requirement for in situ excitation from PLNPs and high selectivity from the aptamer, allowing sensitive and autofluorescence-free determination of kanamycin in food samples.

EXPERIMENTAL SECTION

Chemicals and Materials. All reagents are of analytical grade unless otherwise specified and used as received without purification. $Ga(NO_3)_3{\cdot}XH_2O$ (99.9%), $Zn(NO_3)_2{\cdot}6H_2O$ (99%), $Cr(NO_3)_3{\cdot}9H_2O$ (99.99%), *N*,*N*-dimethylformamide, 3-aminopropyltriethoxysilane, 1,6-hexanediamine, acetic acid, 4-(2-hydroxyethyl)-1-piperazineethanesulfonic acid (HEPES), $FeCl_3{\cdot}6H_2O$, glycol, kanamycin, chloramphenicol, tetracycline, gentamycin sulfate, and sulfamethazine sodium salt were obtained from Aladdin (Shanghai, China). Sulfo-*N*-succinimidyl 4-(maleimidomethyl) cyclohexane-1-carboxylate ester sodium salt (Sulfo-SMCC) was acquired from Macklin (Shanghai, China). Sulfhydryl-modified kanamycin aptamer and its part cDNA (Table S1) were obtained from Shanghai Sangon Biological Science & Technology (Shanghai, China). The PALL PES filter membrane (0.22 μm) was provided by Ameritech Scientific (Laguna Hill, CA). A certified reference material (P30099) (milk powder) was obtained from Guangzhou Puen Scientific Instrument Co., Ltd (Guangzhou, China). Phosphate-buffered saline (PBS) buffer solution (10 mM NaH_2PO_4–Na_2HPO_4, 100 mM NaCl, pH 7.4) was used as the working buffer. Wahaha ultrapure water (Hangzhou, China) was used throughout the work.

Instrumentation. The size and morphology of the prepared nanoparticles was characterized on a model JEM-2100 transmission electron microscope (TEM) (JEOL, Japan). X-ray diffraction (XRD) patterns were recorded on a D2 PHASER powder diffractometer with a Cu Kα radiation source (Bruker, Germany). UV–vis spectra were acquired on a UV-3600PLUS spectrophotometer (Shimadzu, Japan). Hydrodynamic diameter and zeta potential were measured on a Nano ZS Zeta sizer with 633 nm He–Ne laser (Malvern, UK). PL measurements were carried out on an F-7000 fluorometer (Hitachi, Japan) in the phosphorescence mode. Fourier transform infrared spectra (FT-IR) were collected on an IS10 FT-IR spectrometer (Nicolet, USA) in the range of 500–4000 cm^{-1}. The magnetic property was studied by using the PPMS-9 Physical Property Measurement System (California, USA).

Synthesis of Aptamer-Modified Fe_3O_4. Amine-functionalized Fe_3O_4 (MNPs-NH_2) was synthesized based on previous methods.[30] 3 mg MNPs-NH_2 and 0.5 mg Sulfo-SMCC were dispersed in HEPES buffer (3 mL, 10 mM, pH 7.2) for 5 min ultrasonication. The mixture was incubated with 2 h of gentle shaking at room temperature. After magnetic separation, the resulting maleimide-activated MNPs-NH_2 was washed three times with pure water and dispersed in PBS buffer (3 mL). MNPs-apt were prepared by incubating the aptamer (3 nmol) and the above MNPs-NH_2 solution with room-temperature shaking overnight. The prepared MNPs-apt were collected via magnetic separation and rinsed three times with PBS buffer to remove the excessive aptamer. The resulting MNPs-apt were finally re-dispersed in PBS buffer before use.

Preparation of cDNA-Functionalized $ZnGa_2O_4$:Cr. $ZnGa_2O_4$:Cr PLNPs was prepared via a direct aqueous-phase approach.[31] Amino-functionalized PLNPs (PLNPs-NH_2) were obtained based on our previous report.[32] Maleimide-activated PLNPs-NH_2 solution was prepared by following the same procedure for MNPs-NH_2 solution. The resulting maleimide-activated PLNPs-NH_2 were separated by centrifugation, rinsed with ultrapure water, and dispersed in 3 mL of PBS buffer. The above maleimide-activated PLNPs-NH_2 solution reacted with cDNA (3 nmol) under shaking at room temperature overnight. The prepared PLNPs-cDNA was separated via centrifugation and rinsed with PBS buffer to remove excessive cDNA. The resulting PLNPs-cDNA were finally re-dispersed in PBS buffer before use.

Fabrication of MNPs-apt@PLNPs-cDNA Aptasensor. The aptasensor was fabricated as follows: the mixture solution of PLNPs-cDNA (1 mg mL^{-1}, 200 μL) and MNPs-apt (1.5 mg mL^{-1}, 200 μL) in PBS buffer was adjusted to 1 mL by adding PBS buffer for 2 h hybridization. The final complex MNPs-apt@PLNPs-cDNA were collected via magnetic separation, rinsed with PBS buffer, and re-suspended in 1 mL PBS buffer.

Preparation of Milk, Honey, and Milk Powder Samples. Ultrahigh-temperature processing (UHT) milk, pasteurized milk, fresh milk, pagoda flower honey, clover honey, honey of various flowers and infant milk powder, adult nutrition milk powder, and student nutrition milk powder were collected from Taobao and a local supermarket. The samples were spiked with kanamycin standard solutions at final concentrations of 0.5 and 1 $\mu g\ kg^{-1}$ before sample preparation for recovery experiments. The milk samples were treated as described in a previous publication.[33] Briefly, 2.5 g milk samples were diluted in 10 mL pure water and the mixture was adjusted to pH 4.6 by dropwise adding acetic acid (20%, v/v) to precipitate proteins. The samples were centrifugated at 10,000 rpm 15 min to remove the denatured precipitated proteins and adjusted to pH 7 by added solution NaOH (1 M). The obtained solution was adjusted to 10 mL with pure water after filtered through a 0.22 μm filter membrane. 2.5 g of milk powder samples was dissolved in 10 mL pure water and then treated in the same way for milk samples. 2.5 g of honey samples was diluted in 10 mL pure water and vortexed vigorously for 2 min and centrifugated at 10,000 rpm for 15 min. After centrifugation, the samples were collected and filtered by a 0.22 μm filter membrane. The solution was adjusted to 10 mL before analysis.

https://dx.doi.org/10.1021/acs.analchem.0c04648
Anal. Chem. 2021, 93, 2589–2595

Scheme 1. Illustration of the Design and Principle of the MNPs-apt@PLNPs-cDNA Aptasensor for Kanamycin

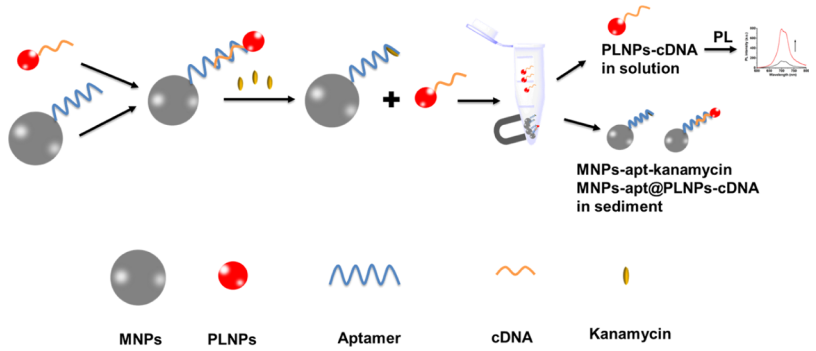

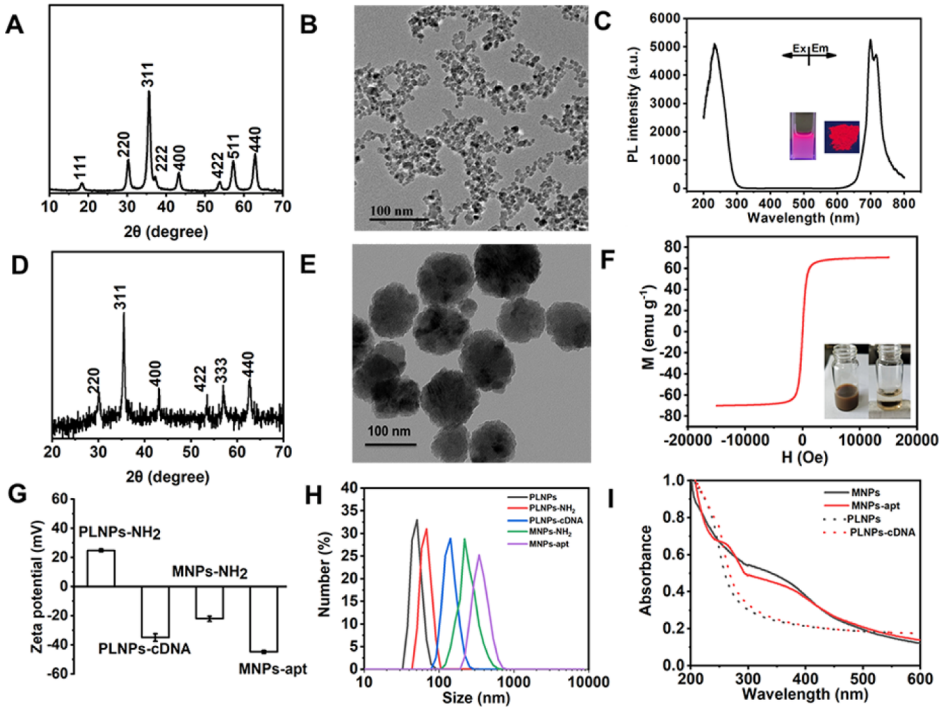

Figure 1. (A) XRD pattern of PLNPs. (B) TEM image of PLNPs. (C) Excitation (em. 700 nm) and emission (ex. 254 nm) spectra of PLNPs aqueous solution (1 mg mL^{-1}). The inset refers to the picture of the as-prepared PLNP solution (left) and powder (right) under UV excitation. (D) XRD pattern of MNPs-NH_2. (E) TEM image of MNPs-NH_2. (F) Room-temperature magnetization curves of obtained MNPs. Inset: photo of the MNPs-NH_2 before (left) and after (right) exposure to an external magnetic field. (G) Zeta potential of PLNPs-NH_2, PLNPs-cDNA, MNPs-NH_2, and MNPs-apt in PBS (1 mM, pH 7.4). (H) Hydrodynamic size distribution of PLNPs, PLNPs-NH_2, PLNPs-cDNA, MNPs-NH_2, and MNPs-apt. (I) UV−vis absorption spectra of PLNPs and MNPs before and after cDNA and aptamer conjugation.

2.5 g of certified reference milk powder was treated the same as milk powder and diluted five times before analysis.

Determination of Kanamycin. 20 μL of kanamycin standard solution or the sample solution was mixed with 180 μL of MNPs-apt@PLNPs-cDNA (0.3 mg mL^{-1}). The mixture solution was made to 400 μL with PBS buffer and incubated with gentle shaking for 90 min. The unreactive MNPs-apt@PLNPs-cDNA and the MNPs-apt-kanamycin were separated by magnetic separation, while the released PLNPs-cDNA were left in the solution. The PL intensity at 700 nm of the solution was measured for the determination of kanamycin on the fluorometer in the phosphorescence mode (excitation at 254 nm, slit widths for excitation and emission, 10 nm).

RESULTS AND DISCUSSION

Design of the PL Aptasensor. The design of the autofluorescence-free luminescent aptasensor for kanamycin detection based on PLNPs-cDNA and MNPs-apt is illustrated in Scheme 1. Here, we apply PLNPs as the luminescence source because the PL of PLNPs can be detected without in situ excitation to eliminate autofluorescence interference in fluorescence detection. To take the advantages of the facile separation of MNPs and the specificity of aptamer, the sulfhydryl-modified kanamycin aptamer is immobilized on MNPs-NH_2, while the cDNA is linked to PLNPs-NH_2 with Sulfo-SMCC as the bifunctional cross-linker to achieve specific affinity.[34] The aptamer is able to hybridize with the cDNA to form the MNPs-apt@PLNPs-cDNA aptosensor. In the presence of kanamycin, the aptamer preferentially binds with kanamycin; thus, MNPs-apt@PLNPs-cDNA is dissociated to release PLNPs-cDNA and MNPs-apt-kanamycin are formed. As the result, only the released PLNPs-cDNA is still left in the solution to give the kanamycin concentration-dependent PL intensity. The developed MNPs-apt@PLNPs-cDNA aptasensor gives the

https://dx.doi.org/10.1021/acs.analchem.0c04648
Anal. Chem. 2021, 93, 2589−2595

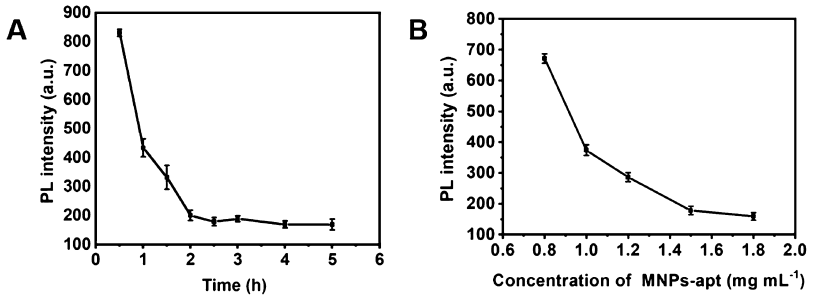

Figure 2. (A) Effect of hybridization time on the PL intensity of PLNPs-cDNA in solution (MNPs-apt: 1.5 mg mL^{-1}, PLNPs-cDNA: 1 mg mL^{-1}). (B) Effect of the concentration of MNPs-apt on the PL intensity of PLNPs-cDNA in solution (1 mg mL^{-1}) (hybridization time, 2 h).

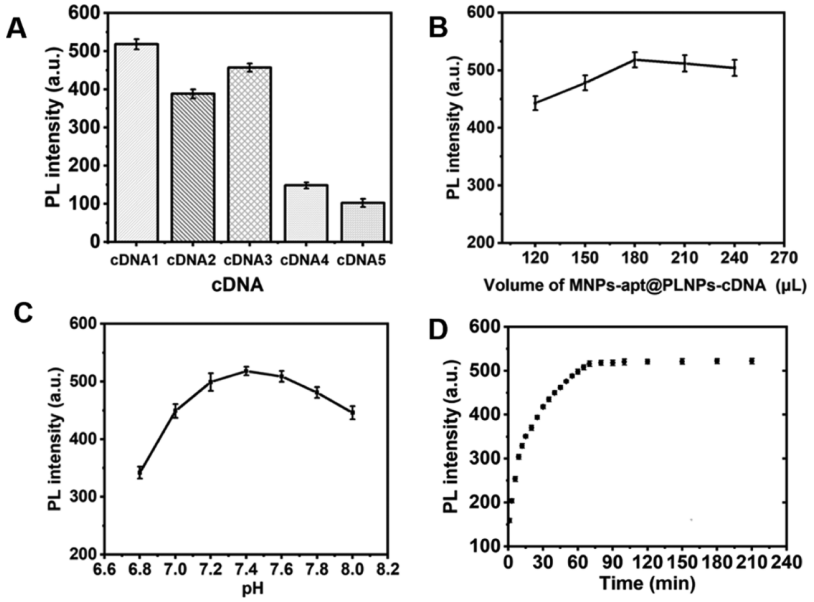

Figure 3. (A) Influence of cDNA on the increased PL intensity in solution after magnetic separation with kanamycin detection concentration at 100 pg mL^{-1}. (B) Effect of the volume of MNPs-apt@PLNPs-cDNA (0.3 mg mL^{-1}) on the increased PL intensity in solution after magnetic separation with kanamycin at 100 pg mL^{-1}. (C) Effect of pH on in solution after magnetic separation. (D) Kinetic curves for the aptasensor. MNPs-apt@PLNPs-cDNA, 0.3 mg mL^{-1}; kanamycin, 100 pg mL^{-1}.

integrated advantages of the unique PL property of PLNPs, the rapid magnetic separation, and the specificity of the aptamer to allow sensitive and autofluorescence-free determination of kanamycin.

Characterization of PLNPs-cDNA and MNPs-apt. The as-prepared PLNPs possess high crystallinity and indexed diffraction peaks of cubic $ZnGa_2O_4$ (JCPDS 38-1240), confirming the characteristic cubic spinel structure (Figure 1A). The PLNPs were well-dispersed with uniform size of the diameter of 7.97 ± 0.63 nm (Figure 1B). The excitation spectra of the PLNPs covered a spectral region of 220−280 nm, and the NIR emission peak was located at 700 nm ($^2E-{}^4A_2$ transition) (Figure 1C).[21] PLNPs show strong emission in both solution and solid state without aggregation-caused quenching effect as the PL of PLNPs depends on the storage of the excitation energy by holes and electron traps (the inset in Figure 1C). The PL signal of PLNPs lasted over 600 s after 5 min excitation with 254 nm UV light, possessed good long PL features (Figure S1A). PLNPs-NH_2 gave strong absorption bands at 1119 and 1035 cm^{-1} for O−Si−O stretching vibration, suggesting a layer of silica coated on PLNPs. The appearance of the N−H stretching bands at 3416 and 3248 cm^{-1} and the symmetrical and asymmetrical stretching vibration bands of $-CH_2-$ at 2932 and 2884 cm^{-1} confirm the successful amino functionalization of PLNPs (Figure S1B). Amination changed the zeta potential of PLNPs to 24.8 mV, whereas further modification with cDNA shifted the zeta potential to −34.9 mV (in PBS, 1 mM, pH 7.4) (Figure 1G), indicating the successful preparation of PLNPs-cDNA. Furthermore, PLNPs-cDNA gave bigger hydrodynamic size than the bare PLNPs and PLNPs-NH_2 (Figure 1H) and an absorption peak at 260 nm (Figure 1I). The coupling efficiency of cDNA on PLNPS was 29.8% (Figure S2).

The as-prepared MNPs-NH_2 showed indexed XRD peaks of Fe_3O_4 (JCPDS 82-1533) (Figure 1D) and uniform spherical morphology with a diameter of 100 ± 2.69 nm (Figure 1E). The appearance of the Fe−O vibrating band at 583 cm^{-1}, the symmetrical and asymmetrical stretching vibration bands of $-CH_2-$ at 2933 and 2874 cm^{-1}, and the characteristic bands of 1629, 1487, and 873 cm^{-1} for $-NH_2$ group confirm the successful amino functionalization of MNPs (Figure S1C). The saturation magnetization of the prepared MNPs reached 70.2 emu g^{-1} which demonstrated highly magnetic properties of prepared MNPs and the MNPs also exhibited good water dispersibility and good separation effect under the external magnet (Figure 2F). The prepared MNPs-apt possessed a zeta potential of −43.7 mV (in PBS, 1 mM, pH 7.4) because of the

https://dx.doi.org/10.1021/acs.analchem.0c04648
Anal. Chem. 2021, 93, 2589−2595

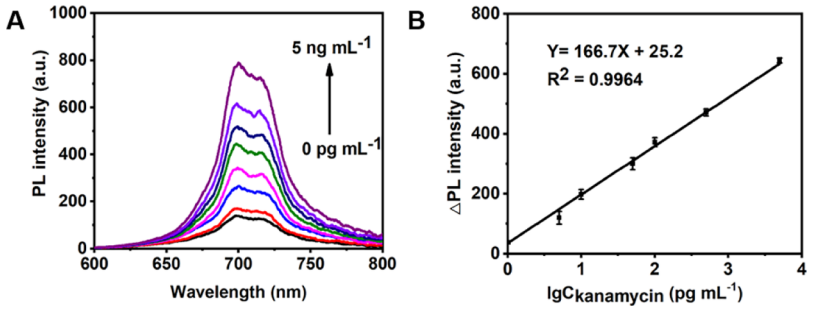

Figure 4. (A) Change in the PL signal in solution after magnetic separation with the concentration of kanamycin. (B) Plot of ΔPL intensity in solution after magnetic separation against the logarithm of kanamycin concentration in the range of 1 pg mL^{-1} to 5 ng mL^{-1}.

phosphoric acid skeleton of the aptamer (Figure 1G). Besides, MNPs-apt possessed bigger hydrodynamic size than MNPs-NH_2 (Figure 1H). The appearance of the UV absorption peak at 260 nm in the UV−vis spectrum of MNPs-apt shows the successful modification of aptamer on the surface of MNPs (Figure 1I). The coupling efficiency of the aptamer on MNPs was calculated to be 23.6% (Figure S2). The content of the aptamer on the MNPs was 6.79 ± 0.04 $\mu g\ mg^{-1}$.

Optimization of the Preparation of MNPs-apt@PLNPs-cDNA. The effects of reaction time and MNPs-apt concentration on the hybridization of MNPs-apt and PLNPs-cDNA were studied with 1 mg mL^{-1} of PLNPs-cDNA. The influence of reaction time on the PL intensity in solution was studied with 1.5 mg mL^{-1} of MNPs-apt and 1 mg mL^{-1} of PLNPs-cDNA. As the DNA hybridization time increased, the PL signal in solution after magnetic separation gradually decreased, then levelled off after 2 h, suggesting that 2 h was sufficient for the full hybridization of MNPs-apt and PLNPs-cDNA (Figure 2A). The PL intensity in solution after magnetic separation gradually decreased as MNPs-apt concentration increased because of the formation of MNPs-apt@PLNPs-cDNA (Figure 2B). Considering that excessive MNPs-apt would bind to the target and result in a decrease in sensitivity, a MNPs-apt concentration of 1.5 mg mL^{-1} was selected.

Optimization of Kanamycin Sensing. It is important to select cDNA for kanamycin to displace PLNPs-cDNA from the MNPs-apt@PLNPs-cDNA. Therefore, the hybridization length and the position complementary of cDNA to the aptamer on MNPs were optimized. To this end, the PL signal of the released PLNPs-cDNA was used as an indicator for cDNA optimization. The results show that cDNA1 which includes 11 bases was better than the other cDNA studied as it gave the highest PL signal (Figure 3A). cDNA4 with eight bases was too short to fully conjugate the aptamer in MNPs-apt, while cDNA5 with 14 bases were too long, making the target difficult to replace PLNPs-cDNA from the composite. cDNA2 and cDNA3 which also consist of 11 bases as cDNA1 but with different positions complementary to the aptamer gave a lower PL signal than DNA1 because of steric hindrance. The effect of the volume of MNPs-apt@PLNPs-cDNA solution (0.3 mg mL^{-1}) on the detection of 100 pg mL^{-1} kanamycin was investigated at pH 7.4. PL intensity in solution after magnetic separation increased to a maximum at 180 μL of MNPs-apt@PLNPs-cDNA solution and then remained constant with further increase of the volume of MNPs-apt@PLNPs-cDNA solution (Figure 3B). A similar result was also obtained for the detection of kanamycin at 5 ng mL^{-1} (Figure S3). As an appropriate pH environment was necessary to ensure the sensitivity of aptamer for target recognition, we also studied the effect of pH on the PL intensity in solution after magnetic separation when the kanamycin concentration was fixed at 100 pg mL^{-1}. The result shows that pH 7.4 was the best as the aptamer becomes less sensitive under highly acidic or alkaline conditions (Figure 3C).[35]

We tested the effect of kinetic curves between MNPs-apt@PLNPs-cDNA (0.3 mg mL^{-1}) and kanamycin (100 pg mL^{-1}) (Figure 3D). Reaction time is an important parameter for kanamycin to compete for the binding of the aptamer of MNPs-apt@PLNPs-cDNA to release PLNPs-cDNA into solution. PL intensity increased rapidly in the first 60 min and then gradually reached the plateau after 80 min. A reaction time of 90 min was chosen to ensure complete reaction between kanamycin and MNPs-apt@PLNPs-cDNA. The dissociation constant (K_d) for the complex of kanamycin and MNPs-apt@PLNPs-cDNA was determined to be 3.12 nM (Supplementary Methods; Figure S4), which is one time lower than those reported in previous assays,[36] suggesting the high affinity of MNPs-apt@PLNPs-cDNA for kanamycin.

Figures of Merit for the Developed Aptasensor. The analytical performance of the developed aptasensor was evaluated under optimal experimental conditions. The PL intensity in solution after magnetic separation increased with kanamycin concentration (Figure 4A). A linear plot of ΔPL (the change of PL intensity at 700 nm due to kanamycin) against the logarithm of kanamycin concentration was obtained with a determination coefficient (R^2) of 0.9964 in the kanamycin concentration range of 1 pg mL^{-1} to 5 ng mL^{-1} (Figure 4B). The limit of detection (LOD) (3s) was 0.32 pg mL^{-1}, and the relative standard deviation for 11 replicate determinations of 100 pg mL^{-1} kanamycin was 3.1%. The developed aptasensor gave much lower LOD than other nanomaterials methods for kanamycin determination (Table S2).

Selectivity of the Developed Aptasensor. To examine the specificity of the proposed aptasensor for kanamycin (KAN), spiked samples containing multiple analogues including sulfadiazine (SDZ), gentamicin (GEN), tetracycline (TC), and chloramphenicol (CAP) were analyzed both in PBS buffer and food matrix. The recoveries for spiked 5 ng mL^{-1} of kanamycin in the presence of other analogues at 50 ng mL^{-1} were in the range of 103.8−107.5% (Table S3), showing that the proposed aptasensor possessed high specificity for the determination of kanamycin because of no significant interferences of other antibiotics even with a 10 times higher concentration (Figure 5).

The selectivity for the proposed aptasensor for kanamycin was also studied in the matrix of the food sample (Figure S5). The recoveries for spiked kanamycin in the presence of other analogues were in the range of 98.4−103.1% in the pasteurized milk sample, 97.1−101% in the pagoda flower honey sample,

https://dx.doi.org/10.1021/acs.analchem.0c04648
Anal. Chem. 2021, 93, 2589−2595

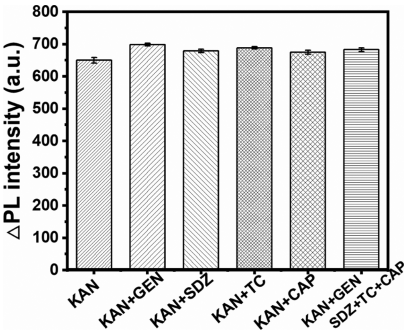

Figure 5. Selectivity for the detection of kanamycin (KAN). Kanamycin, 5 ng mL^{-1}; sulfadiazine (SDZ), gentamicin (GEN), tetracycline (TC), and chloramphenicol (CAP), 50 ng mL^{-1}.

and 98.7−102.7% in the adult nutrition milk powder sample. The result verified that the proposed aptasensor possessed excellent resistance of the food matrix because of the autofluorescence-free nature of PLNPs.

Method Validation and Application to Real Sample Analysis. The proposed aptasensor was validated by analyzing a certified reference material (P30099) (milk powder) for kanamycin. The good agreement between the determined concentration of kanamycin by our aptasensor assay [1127.6 ± 9.0 $\mu g\ kg^{-1}$ (n = 5)] and the certified value (1128.9 ± 4.0 $\mu g\ kg^{-1}$) demonstrates the accuracy of the developed aptasensor. The proposed aptasensor was then applied to the determination of kanamycin in milk, honey, and milk powder samples. The recoveries for spiked kanamycin in these samples were in the range of 95.4−106.3%, indicating no significant interferences encountered for kanamycin determination (Table 1). Kanamycin was detected only in a fresh milk sample (0.248 ± 0.003 $\mu g\ kg^{-1}$). Kanamycin in all the studied samples was well below the maximum allowable level in the national standard (150 $\mu g\ kg^{-1}$ for milk).

CONCLUSIONS

We have reported a functionalized PLNP-based aptasensor for sensitive, selective, and autofluorescence-free determination of kanamycin in food samples. The proposed aptasensor not only allows effective elimination of interference from the food matrix but also permits easy extension to other analytes by simply replacing the aptamer, showing a great promise as a universal aptasensor platform for selective, sensitive, and autofluorescence-free detection of hazardous analytes in food samples.

ASSOCIATED CONTENT

Supporting Information

The Supporting Information is available free of charge at https://pubs.acs.org/doi/10.1021/acs.analchem.0c04648.

Additional figures for the luminescence decay curve of PLNPs, FT-IR spectra of PLNPs and PLNPs-NH_2, FT-IR spectrum of MNPs-NH_2, calibration curves for kanamycin aptamer and cDNA, UV−vis spectra of kanamycin aptamer solution before and after coupling to MNPs, UV−vis spectra of cDNA solution before and after coupling to PLNPs, effect of the volume of MNPs-apt@PLNPs-cDNA on ΔPL in solution after magnetic separation for the determination of kanamycin, PL intensity in solution after magnetic separation in the

Table 1. Analytical Results for Determination of Kanamycin in Food Samples[a]

samples	spiked kanamycin ($\mu g\ kg^{-1}$)	concentration determined ($\mu g\ kg^{-1}$, mean ± s, n = 3)	recovery (%, mean ± s, n = 3)
UHT milk	0	ND	
	0.5	0.527 ± 0.022	105.4 ± 4.5
	1.0	1.038 ± 0.058	103.8 ± 5.8
pasteurized milk	0	ND	
	0.5	0.485 ± 0.030	97.1 ± 6.0
	1.0	1.053 ± 0.081	105.3 ± 8.2
fresh milk	0	0.248 ± 0.003	
	0.5	0.738 ± 0.010	98.7 ± 2.1
	1.0	1.307 ± 0.012	104.7 ± 2.0
pagoda flower honey	0	ND	
	0.5	0.478 ± 0.010	95.6 ± 2.0
	1.0	0.997 ± 0.089	99.7 ± 8.9
clover honey	0	ND	
	0.5	0.492 ± 0.021	98.4 ± 4.2
	1.0	1.050 ± 0.051	105.2 ± 5.1
honey of various flowers	0	ND	
	0.5	0.477 ± 0.035	95.4 ± 7.1
	1.0	1.040 ± 0.097	104.0 ± 9.7
infant milk powder	0	ND	
	0.5	0.528 ± 0.049	105.6 ± 9.8
	1.0	0.981 ± 0.021	98.1 ± 2.1
adult nutrition milk powder	0	ND	
	0.5	0.532 ± 0.015	106.3 ± 3.0
	1.0	0.964 ± 0.038	96.4 ± 3.8
student nutrition milk powder	0	ND	
	0.5	0.515 ± 0.033	103.1 ± 6.5
	1.0	1.014 ± 0.048	101.4 ± 4.8

[a]ND: not detected.

https://dx.doi.org/10.1021/acs.analchem.0c04648
Anal. Chem. 2021, 93, 2589−2595

presence of increasing concentrations of kanamycin, interference of other antibiotics on the determination of Kanamycin in the food matrix, additional tables for the sequence of the kanamycin aptamer and cDNA, recoveries for determination of kanamycin in the presence of other analogues, comparison of the developed aptasensor with other reported methods for the determination of kanamycin (PDF)

AUTHOR INFORMATION

Corresponding Author

Xiu-Ping Yan − *State Key Laboratory of Food Science and Technology, Jiangnan University, Wuxi 214122, China; International Joint Laboratory on Food Safety, Institute of Analytical Food Safety, School of Food Science and Technology, and Key Laboratory of Synthetic and Biological Colloids, Ministry of Education, Jiangnan University, Wuxi 214122, China;* orcid.org/0000-0001-9953-7681; Phone: +86-510-85916732; Email: xpyan@jiangnan.edu.cn

Authors

Bei-Bei Wang − *State Key Laboratory of Food Science and Technology, Jiangnan University, Wuxi 214122, China; International Joint Laboratory on Food Safety and Institute of Analytical Food Safety, School of Food Science and Technology, Jiangnan University, Wuxi 214122, China*

Xu Zhao − *State Key Laboratory of Food Science and Technology, Jiangnan University, Wuxi 214122, China; International Joint Laboratory on Food Safety and Institute of Analytical Food Safety, School of Food Science and Technology, Jiangnan University, Wuxi 214122, China;* orcid.org/0000-0001-8000-9045

Li-Jian Chen − *State Key Laboratory of Food Science and Technology, Jiangnan University, Wuxi 214122, China; International Joint Laboratory on Food Safety and Institute of Analytical Food Safety, School of Food Science and Technology, Jiangnan University, Wuxi 214122, China;* orcid.org/0000-0001-8671-8766

Cheng Yang − *State Key Laboratory of Food Science and Technology, Jiangnan University, Wuxi 214122, China; International Joint Laboratory on Food Safety and Institute of Analytical Food Safety, School of Food Science and Technology, Jiangnan University, Wuxi 214122, China*

Complete contact information is available at: https://pubs.acs.org/10.1021/acs.analchem.0c04648

Notes

The authors declare no competing financial interest.

ACKNOWLEDGMENTS

The authors appreciate the financial supports from the National Natural Science Foundation of China (nos. 21934002, 21804056, and 21804057), the National First-class Discipline Program of Food Science and Technology (no. JUFSTR20180301), and the Program of "Collaborative Innovation Center of Food Safety and Quality Control in Jiangsu Province".

REFERENCES

(1) Huang, S.; Gan, N.; Zhang, X.; Wu, Y.; Shao, Y.; Jiang, Z.; Wang, Q. *Biosens. Bioelectron.* **2019**, *128*, 113−121.
(2) Robati, R. Y.; Arab, A.; Ramezani, M.; Langroodi, F. A.; Abnous, K.; Taghdisi, S. M. *Biosens. Bioelectron.* **2016**, *82*, 162−172.
(3) Rowe, A. A.; Miller, E. A.; Plaxco, K. W. *Anal. Chem.* **2010**, *82*, 7090−7095.
(4) Yang, Q.; Hong, J.; Wu, Y.-X.; Cao, Y.; Wu, D.; Hu, F.; Gan, N. *ACS Appl. Mater. Interfaces* **2019**, *11*, 41506−41515.
(5) Bi, H.; Wu, Y.; Wang, Y.; Liu, G.; Ning, G.; Xu, Z. *J. Electroanal. Chem.* **2020**, *870*, 114216.
(6) Wang, Q.; Zhao, W.-M. *Sens. Actuators, B* **2018**, *269*, 238−256.
(7) Zeng, R.; Luo, Z.; Su, L.; Zhang, L.; Tang, D.; Niessner, R.; Knopp, D. *Anal. Chem.* **2019**, *91*, 2447−2454.
(8) Khan, S.; Miguel, E. M.; de Souza, C. F.; da Silva, A. R.; Aucélio, R. Q. *Sens. Actuators, B* **2017**, *246*, 444−454.
(9) Su, P.; Chen, X.; He, Z.; Yang, Y. *Chem. Res. Chin. Univ.* **2017**, *33*, 876−881.
(10) Nasim, A.; Aslam, B.; Javed, I.; Ali, A.; Muhammad, F.; Raza, A.; Sindhu, Z.-u. -D. *J. Sci. Food Agric.* **2016**, *96*, 1284−1288.
(11) Jiang, Y.; Sun, D.-W.; Pu, H.; Wei, Q. *Talanta* **2019**, *197*, 151−158.
(12) Lin, X.; Su, J.; Lin, H.; Sun, X.; Liu, B.; Kankala, R. K.; Zhou, S.-F. *Talanta* **2019**, *202*, 452−459.
(13) Dijkstra, J. A.; Voerman, A. J.; Greijdanus, B.; Touw, D. J.; Alffenaar, J. W. C. *Antimicrob. Agents Chemother.* **2016**, *60*, 4646−4651.
(14) Li, C.; Zhang, Y.; Eremin, S. A.; Yakup, O.; Yao, G.; Zhang, X. *Food Chem.* **2017**, *227*, 48−54.
(15) Feng, D.; Tan, X.; Wu, Y.; Ai, C.; Luo, Y.; Chen, Q.; Han, H. *Biosens. Bioelectron.* **2019**, *129*, 100−106.
(16) Li, F.; Guo, Y.; Wang, X.; Sun, X. *Biosens. Bioelectron.* **2018**, *115*, 7−13.
(17) Zhou, Y.; Li, F.; Wu, H.; Chen, Y.; Yin, H.; Ai, S.; Wang, J. *Sens. Actuators, B* **2019**, *296*, 126664.
(18) Ou, X.; Chen, Y.; Xie, L.; Chen, J.; Zan, J.; Chen, X.; Hong, Z.; He, Y.; Li, J.; Yang, H. *Anal. Chem.* **2019**, *91*, 10149−10155.
(19) Ou, X.-Y.; Guo, T.; Song, L.; Liang, H.-Y.; Zhang, Q.-Z.; Liao, J.-Q.; Li, J.-Y.; Li, J.; Yang, H.-H. *Anal. Chem.* **2018**, *90*, 6992−6997.
(20) Wang, J.; Ma, Q.; Hu, X.-X.; Liu, H.; Zheng, W.; Chen, X.; Yuan, Q.; Tan, W. *ACS Nano* **2017**, *11*, 8010−8017.
(21) Zhou, Z.; Zheng, W.; Kong, J.; Liu, Y.; Huang, P.; Zhou, S.; Chen, Z.; Shi, J.; Chen, X. *Nanoscale* **2017**, *9*, 6846−6853.
(22) Li, Y.-J.; Yan, X.-P. *Nanoscale* **2016**, *8*, 14965−14970.
(23) Wang, J.; Li, J.; Yu, J.; Zhang, H.; Zhang, B. *ACS Nano* **2018**, *12*, 4246−4258.
(24) Wu, S.-Q.; Yang, C.-X.; Yan, X.-P. *Adv. Funct. Mater.* **2017**, *27*, 1604992.
(25) Zhao, X.; Chen, L.-J.; Zhao, K.-C.; Liu, Y.-S.; Liu, J.-l.; Yan, X.-P. *TrAC, Trends Anal. Chem.* **2019**, *118*, 65−72.
(26) Jiang, Y.-Y.; Zhao, X.; Chen, L.-J.; Yang, C.; Yin, X.-B.; Yan, X.-P. *Talanta* **2020**, *218*, 121101.
(27) Khatibi, S. A.; Hamidi, S.; Siahi-Shadbad, M. R. *Crit. Rev. Food Sci. Nutr.* **2020**, *50*, 1−16.
(28) Chen, J.; Ying, G.-G.; Deng, W.-J. *J. Agric. Food Chem.* **2019**, *67*, 7569−7586.
(29) You, F.; Wei, J.; Cheng, Y.; Wen, Z.; Ding, C.; Guo, Y.; Wang, K. *J. Hazard. Mater.* **2020**, *398*, 122944.
(30) Wang, L.; Bao, J.; Wang, L.; Zhang, F.; Li, Y. *Chem.—Eur. J.* **2006**, *12*, 6341−6347.
(31) Li, Z.; Zhang, Y.; Wu, X.; Huang, L.; Li, D.; Fan, W.; Han, G. *J. Am. Chem. Soc.* **2015**, *137*, 5304−5307.
(32) Abdukayum, A.; Chen, J.-T.; Zhao, Q.; Yan, X.-P. *J. Am. Chem. Soc.* **2013**, *135*, 14125−14133.
(33) Xu, C.; Ying, Y.; Ping, J. *Microchim. Acta* **2019**, *186*, 448.
(34) Zhao, Z.; Meng, H.; Wang, N.; Donovan, M. J.; Fu, T.; You, M.; Chen, Z.; Zhang, X.; Tan, W. *Angew. Chem., Int. Ed.* **2013**, *52*, 7487−7491.
(35) Hianik, T.; Ostatná, V.; Sonlajtnerova, M.; Grman, I. *Bioelectrochemistry* **2007**, *70*, 127−133.
(36) Sharma, T. K.; Ramanathan, R.; Weerathunge, P.; Mohammadtaheri, M.; Daima, H. K.; Shukla, R.; Bansal, V. *Chem. Commun.* **2014**, *50*, 15856−15859.